JOC The Journal of Organic Chemistry

Note

pubs.acs.org/joc

π-Complexation in Nickel-Catalyzed Cross-Coupling Reactions

S. Kyle Sontag,[†,∥] Jenna A. Bilbrey,[†,‡,∥] N. Eric Huddleston,[†] Gareth R. Sheppard,[†] Wesley D. Allen,*[,†,‡] and Jason Locklin*[,†,§]

[†]Department of Chemistry, [‡]Center for Computational Chemistry, and [§]College of Engineering, University of Georgia, Athens, Georgia 30602, United States

Supporting Information

ABSTRACT: The kinetic isotope effect (KIE) is used to experimentally elucidate the first irreversible step in oxidative addition reactions of a zerovalent nickel catalyst to a set of haloarene substrates. Halogenated *o*-methylbenzene, dimethoxybenzene, and thiophene derivatives undergo intramolecular oxidative addition through irreversible π-complexation. Density functional theory computations at the B3LYP-D3/TZ2P-LANL2TZ(f)-LANL08d level predict η^2-bound π-complexes are generally stable relative to a solvated catalyst plus free substrate and that ring-walking of the Ni(0) catalyst and intramolecular oxidative addition are facile in these intermediates.

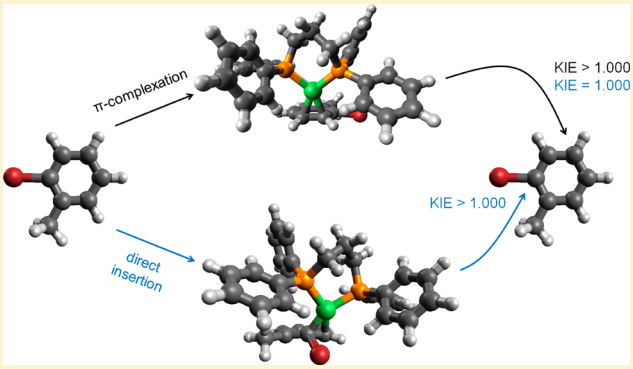

The Kumada−Tamao−Corriu (KTC) reaction is commonly used for carbon−carbon cross-coupling in small molecule synthesis.[1] In such reactions, a zerovalent nickel catalyst undergoes a fundamental catalytic cycle involving oxidative addition (OA) to a reactive substrate, transmetalation with a Grignard reagent, and reductive elimination to form a carbon−carbon bond. The OA reaction, which initiates the catalytic cycle by conversion of starting materials to reactive intermediates, is known to be a two-step process with the transition metal catalyst first undergoing initial complexation with the substrate followed by nickel insertion.[2] The resulting intermediate is generally stable and proceeds as the substrate for transmetalation in organometallic reactions. Some computational work has examined the role of oxidative addition for zerovalent group 10 metals in various cross-coupling reactions, mostly focusing on the nickel insertion step with limited substrates.[3]

In the KTC system, a π-complex is formed between the Ni(0) d-orbitals and the antibonding π-orbitals of the aryl substrate prior to halogen bond cleavage.[4] For an aryl bromide substrate initial π-complexation drives preferential bond activation even in the presence of a more reactive aryl iodide substrate.[5] This selectivity suggests that the Ni(0) species does not dissociate from the π-complex and must move along the conjugated framework (ring-walk) toward the active carbon−halogen site. Recently, small molecule competition reactions by the McNeil group have shown that intramolecular oxidative addition occurs.[6]

The nickel-mediated cross-coupling reaction is often used in the synthesis of near monodisperse, conjugated polymers.[7] The π-complexation of zerovalent nickel with aromatic substrates plays a critical role in polymerization control, and weak association leads to uncontrolled polymerization.[8] The Ni(0) catalyst "chain-walks" along the aromatic polymer backbone, and the nature of the aromatic system can alter this chain-walking phenomenon. A recent review by the McNeil group discusses our limited knowledge of the binding and whether the substrate is in η^2-, η^4-, or η^6-coordination with Ni(0).[9] An experimental and theoretical understanding of the interaction of Ni(0) catalysts with aromatic substrates promises to provide more efficient, selective catalysts for polymerization.

Though the formation of π-complexes plays an important role in many cross-coupling reactions, isolation or direct observation is often not possible due to the short lifetimes of these metastable species.[10] However, the kinetic isotope effect (KIE) can provide information on the atoms involved in the first irreversible step (FIS) when a catalyst is involved.[2c,3a,11] In reactions such as OA involving bond rearrangements, substitution of heavier isotopes tends to enhance activation barriers and reduce reaction rates.[12] When probing carbon isotope effects, substrates containing the lighter ^{12}C atom will preferentially react, leaving ^{13}C enrichment at the active site in recovered starting material. An increased KIE (>1.000 relative to an internal standard) at an atomic position indicates involvement of this site in the FIS. Carbon-specific KIEs can be quantified by ^{13}C NMR through comparison of ^{13}C ratios in the substrate before and after reaction.[13] In this case, deliberate isotopic labeling is unnecessary because the natural abundance of ^{13}C is sufficient for high-field NMR methods.

In this report, we perform KIE experiments on various haloarene derivatives to elucidate the OA mechanism. Aryl halides are coupled with alkyl or aryl magnesium halides using

Received: October 10, 2013
Published: February 3, 2014

dx.doi.org/10.1021/jo402259z | J. Org. Chem. 2014, 79, 1836−1841

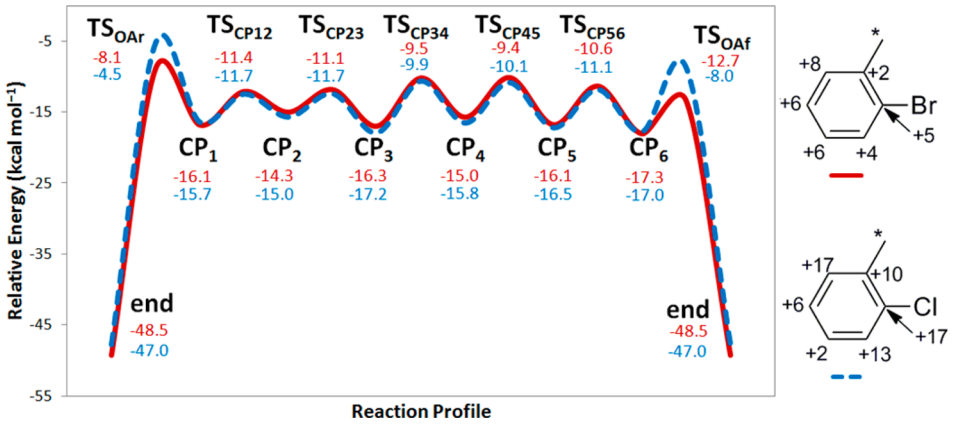

Figure 1. Computed reaction profile for intramolecular oxidative addition of Ni(dppp) with *o*-bromotoluene (solid red) and *o*-chlorotoluene (dashed blue). Energies relative to THF-Ni(dppp) + free substrate are listed for each step. Experimental KIEs are given using the shorthand notation defined in the text with an asterisk denoting the internal standard.

dppp-ligated nickel catalysts. Several thiophene derivatives are also investigated to understand Ni(0) interactions with aromatic rings containing a heteroatom. Additionally, reaction pathways were computed using B3LYP-D3/TZ2P-LANL2TZ-(f)-LANL08d density functional theory. Initial π-complexation thermodynamically stabilizes the benzene and thiophene derivatives by up to 17 and 33 kcal mol^{-1}, respectively, relative to the solvated catalyst and free substrate, and all cross-couplings are exothermic with low barriers to OA. Theoretical KIEs for Ni(0) insertion were calculated using simple transition state theory[12] and found to differ from the observed KIEs, providing further evidence that the initial step for all studied substrates is not direct oxidative addition.

To examine substrate influence on the OA reaction, KIEs were measured for a set of haloarenes varying in halogen type (benzene derivatives), added electron-withdrawing groups, and substituent position (thiophene derivatives). Increased KIEs only in the immediate vicinity of the halogenated carbon would indicate that Ni(0) insertion is the first irreversible step and that π-complexation is reversible. Conversely, increased ratios distributed over the aryl ring would imply mechanistic involvement of carbons away from the OA reaction site, suggesting that π-complexation is the FIS, and once the catalyst coordinates to the substrate then intramolecular OA occurs without dissociation of Ni(0). Our measured KIE values are reported in the figures below in a succinct notation. Differences are given with respect to the methyl internal standard, set at 1.000, and are reported as multiples of 0.001. For example, a KIE of +8 corresponds to 1.008 in the standard notation.

The stability of π-complexation varying by halogen type was first investigated for substituted *o*-halotoluenes (Figure 1). The experimental ^{13}C KIE values for the brominated substrate are (+5, +4, +6, +6, +8, +2), while the corresponding KIEs for the chlorinated substrate are (+17, +13, +2, +6, +17, +10). The enlargement in positions away from the site of oxidative addition indicates that π-complexation is the FIS. Intramolecular OA is expected for both species. This matches literature reports confirming chain-growth character in the KTC polymerization.[14]

Modeling the full OA reaction of Ni(dppp) with *o*-bromotoluene reveals that Ni(0) favorably complexes in an η^2 fashion with neighboring sp^2 carbons followed by ring-walking and nickel insertion, as shown in Scheme 1. In the KIE experiments, a free Ni(0) would initially be complexed to the

Scheme 1. Ring-Walking and Forward Nickel Insertion of Ni(dppp) with *o*-Bromotoluene[a]

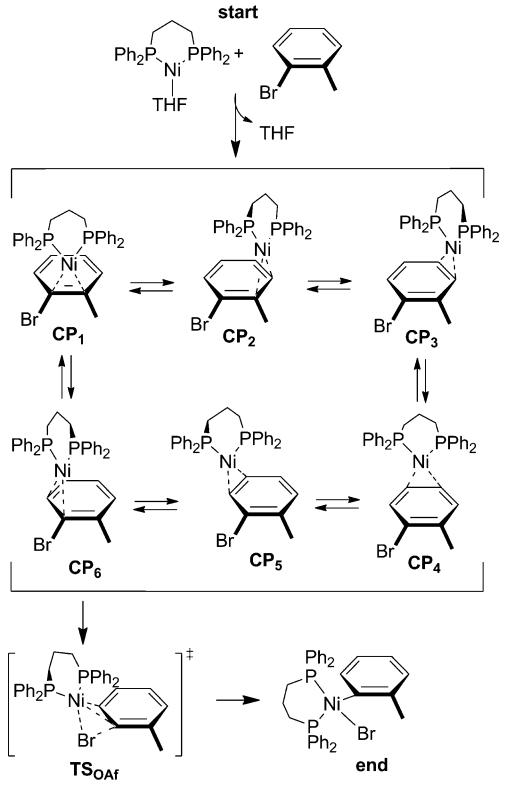

[a]Initial binding can occur at any position (CP_x).

THF solvent.[15] The THF is replaced by the aryl halide substrate at the start of the reaction sequence. This process cannot be described as a single step through a well-defined transition state on the potential energy surface. While theoretical investigation of complicated exchange mechanisms among Ni(0) π-complexes is beyond the scope of this report, the associated thermodynamic effects are accounted for by computing relative energies based on the reaction THF-Ni(dppp) + substrate → substrate-Ni(dppp) + THF.

Figure 1 displays the computed reaction profile for intramolecular OA of Ni(dppp) with the brominated (solid red trace) and chlorinated (dashed blue trace) derivatives.

dx.doi.org/10.1021/jo402259z | J. Org. Chem. 2014, 79, 1836−1841

Initial π-complexation with the substrate provides 14−17 kcal mol^{-1} of thermodynamic stabilization depending on the binding position. All ring-walking steps have low energetic barriers of 3−7 kcal mol^{-1}. Ni(dppp) can migrate around the ring to the active site in either a forward direction away from the methyl substituent or in a reverse direction passing over the methyl moiety. OA occurs via a three-coordinate transition state (TS_{OA}) involving either C1−C6 or C1−C2 for forward and reverse ring-walking, respectively.

The main difference between the bromo- and chlorotoluene substrates is the nickel insertion barrier, which is somewhat higher for the chloro derivative. The insertion barriers in the forward direction are 4.6 and 9.0 kcal mol^{-1} for the bromo and chloro derivatives, while those in the reverse direction are 8.0 and 11.2 kcal mol^{-1}. In the forward ring-walking reaction with the brominated substrate, the barrier for insertion is lower in energy than that of ring-walking, which suggests extremely facile intramolecular oxidative addition. The reaction profiles of Figure 1, especially in the *o*-chlorotoluene case, suggest fast pre-equilibrium between the intermediates, allowing application of the Curtin−Hammett principle[16] or the energetic span model.[17] In particular, the apparent activation energy for nickel insertion in the reverse direction is predicted to be 12.5 kcal mol^{-1}, the difference between the energy of TS_{OAr} and the lowest-energy intermediate CP_6. The thermodynamic driving force for OA after π-complexation exceeds 45 kcal mol^{-1}.

The experimental KIEs for the brominated derivative exhibited sizable enlargement on every aryl carbon, making π-complexation the apparent FIS. In contrast, for the nickel insertion step, our theoretical KIEs for C1 through C6 are (+4, +5, +2, +0, +0, +2) and (+5, +2, +0, +1, +3, +5) for the forward and reverse directions, respectively. The clear disparity between these theoretical values and the observed KIEs supports the conclusion that nickel insertion is not the FIS. For the chlorinated substrate, our theoretical KIEs for nickel insertion in the forward and reverse direction are (+6, +5, +1, −1, +0, +2) and (+8, +1, −1, −1, +2, +4). Again, substantial enlargement is only present on the active carbon and its neighbors, which does not match experiment, indicating nickel insertion is not the FIS.

The addition of methoxy substituents alters the relative energies of the various π-complexes (Figure 2). Instead of all binding positions being of comparable energy, as for the halotoluene derivatives, the unsubstituted site C4 is favored by 6.2 kcal mol^{-1}. While the barriers to ring-walking out of the deepest CP_4 and CP_1 minima are 7−12 kcal mol^{-1}, the others are only 2−5 kcal mol^{-1}. The barrier nickel insertion from the unhindered side is only slightly higher barrier to nickel insertion at 6.8 kcal mol^{-1}. No transition state was located for nickel insertion from the hindered side.

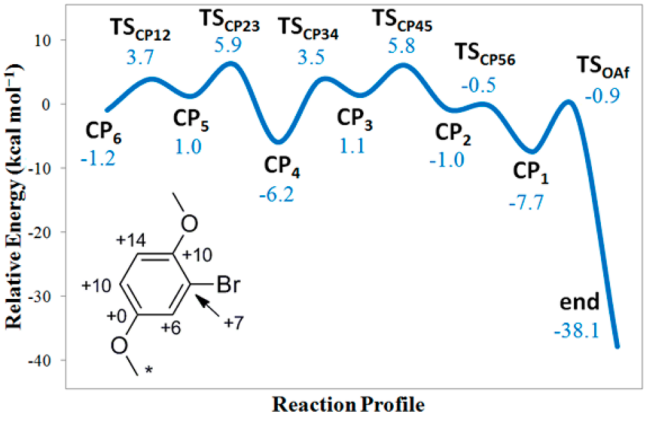

Figure 2. Computed reaction profile for intramolecular oxidative addition of Ni(dppp) with 1-bromo-2,5-dimethoxybenzene. The energies listed for each step are relative to THF-Ni(dppp) + free substrate. Experimental KIEs are inset.

The experimental KIEs (+7, +10, +14, +10, +0, +6) for 1-bromo-2,5-dimethoxybenzene are elevated around the ring. In contrast, the theoretical KIEs for nickel insertion (+3, +2, +1, −1, +0, +0) exhibit noticeably increased values only at the two carbons involved in the three-coordinate OA transition state (C1 and C2). The theoretical KIEs for nickel insertion do not reflect trends in the experimental KIEs, implying π-complexation is the apparent FIS.

Thiophene compounds were investigated to study heteroatom effects on the OA mechanism, which are of relevance in small molecule cross-couplings and conjugated polymers.[7b,18] A key difference between the toluene and thiophene derivatives is the mode of ring-walking. Nickel can complex with toluene derivatives at any adjacent pair of aryl carbons, but thiophene π-complexation only occurs at the C2−C3 and C4−C5 positions, as outlined in Scheme 2. No stationary points were found on the potential energy surface for Ni(dppp) complexed with the sulfur atom of thiophene.

Scheme 2. Intramolecular Oxidative Addition of Ni(dppp) with 2-Bromo-3-methylthiophene

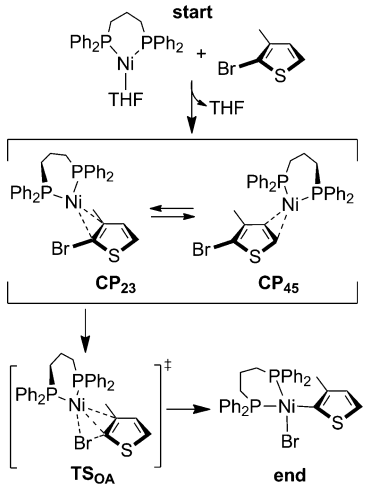

Figure 3 shows the computed reaction profiles and experimental KIEs for bromothiophene derivatives. The substrate 2-bromo-3-methylthiophene has increased KIEs at C4 and C5 of +22 and +12. The lack of an increased KIE at C3 and the much smaller increase at C2 indicate that nickel insertion is not the FIS. When the methyl substituent is in the 5-position, experimental KIEs are spread throughout the ring at (+17, +4, +6, +16). The theoretical KIEs for nickel insertion are (+4, +5, +3, +0) for 2-bromo-3-methylthiophene and (+3, +6, +4, +1) for 2-bromo-5-methylthiophene. This disparity suggests π-complexation is the FIS.

In the 3-methyl and 5-methyl thiophene derivatives, the barriers to forward ring-walking are 14.5 and 13.5 kcal mol^{-1}, respectively, much larger than found in the halogenated toluene derivatives. The corresponding barriers to nickel insertion in

dx.doi.org/10.1021/jo402259z | J. Org. Chem. 2014, 79, 1836−1841

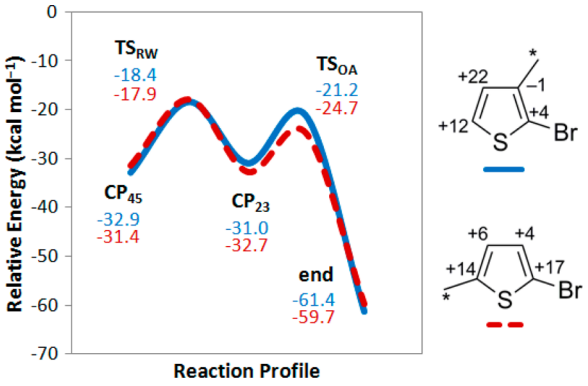

Figure 3. Computed reaction profiles and experimental KIEs for 2-bromo-3-methylthiophene (solid blue trace) and 2-bromo-5-methylthiophene (dashed red trace). Energies are listed for each step relative to THF–Ni(dppp) + free substrate.

the forward direction are 9.8 and 8.0 kcal mol^{-1}, comparable to the bromotoluene values.

In summary, Kumada coupling reactions were carried out here on a collection of halogenated arene derivatives. Experimental and computational methods were combined to elucidate the reactions of zerovalent nickel with aromatic substrates. Kinetic isotope effects (KIEs) were obtained from ^{13}C NMR integrations of starting material before and after cross-coupling. Inverse-gated decoupling allowed for accurate peak integration, and the relaxation agent Cr(acac)$_3$ significantly decreased the NMR acquisition time. Our joint experimental and theoretical analysis indicates that the first irreversible step (FIS) in the oxidative addition of Ni(0) with haloarenes is π-complexation, followed by intramolecular nickel insertion. The observed characteristics of π-complexation are of mechanistic importance in the Kumada catalyst-transfer polymerization of these substrates, as dissociation of the Ni(0) catalyst between the reductive elimination and subsequent oxidative addition step results in a loss of chain-growth behavior. Initial π-complexation is a contributing factor to obtaining a chain-growth polymerization with low dispersity and controlled end groups.

EXPERIMENTAL SECTION

Experimental Methods. *ortho*-Toluene substrates were used in order to aid in cross-coupling reactions.[19] The exchange reagent (RMgCl) for each reaction was selected to allow facile separation of starting material from products and minimize magnesium halogen exchange. The use of *n*-hexyl magnesium chloride as the Grignard reagent ensured the coupled product acquired a significantly higher boiling point than the starting material, allowing ease of separation via distillation. Furthermore, it is well documented that thienyl halides participate in magnesium halogen exchange processes,[20] which give rise to a number of different products and influences KIE values. To minimize this complication, thienyl halide substrates were reacted with thiophen-2-yl magnesium chloride instead of *n*-hexyl magnesium chloride.

The determination of KIEs by NMR requires integration of the ^{13}C spectra for the substrate before reaction and for recovered starting material after reaction. Cr(acac)$_3$ was used as a relaxation agent to lower the half-life (T_1) of nuclear relaxation, which significantly decreased the time necessary to acquire spectra with a signal-to-noise of 1000:1.[21] The pulse width was set to 90°, followed by a relaxation delay of at least five T_1. Nuclear Overhauser effects were suppressed using the inverse gated decoupling technique. The integral values of the peaks before and after reaction were compared, and the KIEs were calculated through the standard ^{13}C formula (see Supporting Information for more details).[13]

1-Bromo-2-methylbenzene. 1-Bromohexane (96 mmol, 15.83 g) was added dropwise to refluxing magnesium metal (96.8 mmol, 2.35 g) in 80 mL of diethyl ether, stirred for 1 h, and then added dropwise to a mixture of *o*-bromotoluene (80 mmol, 13.68 g) and 2 mol % Ni(dppp)Cl$_2$ (1.6 mmol) at 0 °C. The reaction was stirred for 24 h at room temperature, then quenched with 1 M HCl, washed with water (3×) and brine (3×), and dried over MgSO$_4$. Distillation yielded 3.39 g (83% conversion) of starting material, 0.90 g of toluene, and 7.25 g of the coupled product. (A_pP_f) = (3.39 g, 83%); ^{1}H (CDCl$_3$, 300 MHz) δ (ppm): 7.43–7.49 (m, 1H), 7.14–7.16 (m, 1H), 7.08–7.12 (m, 1H), 6.92–6.95 (m, 1H), 2.38 (s, 3H); ^{13}C{^{1}H} (CDCl$_3$, 600 MHz) δ (ppm): 23.1, 125.2, 127.5, 127.6, 131.0, 132.5, 137.9.

1-Chloro-2-methylbenzene. 1-Bromohexane (144 mmol, 23.75 g) was added dropwise to refluxing magnesium metal (145 mmol, 3.53 g) in 100 mL of diethyl ether, stirred for 1 h, then added dropwise to a mixture of *o*-chlorotoluene (120 mmol, 15.19 g) and 2 mol % Ni(dppp)Cl$_2$ (2.4 mmol) at 0 °C, and stirred for 24 h at room temperature. The reaction was quenched with 1 M HCl, washed with water (3×) and brine (3×), and dried over MgSO$_4$. Distillation yielded 1.52 g (90% conversion) of starting material and 16.40 g of coupled product. (A_pP_f) = (1.52 g, 90%); ^{1}H NMR (CDCl$_3$, 300 MHz) δ (ppm): 7.24–7.27 (m, 1H), 7.11–7.14 (m, 1H), 7.05–7.08 (m, 1H), 7.00–7.04 (m, 1H), 2.36 (s, 3H); ^{13}C{^{1}H} (CDCl$_3$, 500 MHz) δ (ppm): 20.4, 127.0, 127.6, 129.5, 131.4, 134.8, 136.4.

1-Bromo-2,5-dimethoxybenzene. 1-Bromohexane (120 mmol, 19.80 g) was added dropwise to refluxing magnesium metal (121 mmol, 2.94 g) in 100 mL of diethyl ether, stirred for 1 h, then added dropwise to a mixture of 2-bromo-1,4-dimethoxybenzene (100 mol, 21.705 g) and 2 mol % Ni(dppp)Cl$_2$ (2 mmol) at 0 °C, and stirred for 24 h at room temperature. The reaction was quenched with 1 M HCl, washed with water (3×) and brine (3×), and dried over MgSO$_4$. Distillation yielded 1.70 g (92% conversion) of starting material, 1.05 g of dimethoxybenzene, and 13.85 g of coupled product. (A_pP_f) = (1.70 g, 92%); ^{1}H NMR (CDCl$_3$, 400 MHz) δ (ppm): 7.10 (s, 1H), 6.79 (s, 2H), 3.80 (s, 3H) 3.72 (s, 3H); ^{13}C{^{1}H} (CDCl$_3$, 600 MHz) δ (ppm): 55.8, 56.8, 111.8, 112.8, 113.4, 119.0, 150.1, 153.9.

2-Bromo-3-methylthiophene. NBS (17.798 g, 100 mmol) was added to 3-methylthiophene (9.818g, 100 mmol) in 100 mL of THF at 0 °C and stirred overnight. The product was purified through an alumina plug with hexanes to yield 13.2 g of 2-bromo-3-methylthiophene (75%). Isopropylmagnesium chloride (92.8 mmol, 46.4 mL) was added dropwise to a solution of 2-bromothiophene (92.8 mmol, 15.12 g) in 100 mL of THF at 0 °C. After complete conversion, the 2-thienylmagnesium chloride was added dropwise to a solution of 2-bromo-3-methylthiophene (92.8 mmol, 16.44 g) and 3 mol % Ni(dppp)Cl$_2$ (2.8 mmol) in 100 mL of THF at 0 °C and stirred overnight. The reaction was quenched with 1 M HCl, and the solvent was removed. The crude mixture was dissolved in hexanes, washed with water (3×), and dried over MgSO$_4$. Distillation yielded 125 mg (98% conversion) of starting material and 12.93 g of coupled product (55 °C, 200 mtorr). (A_pP_f) = (125 mg, 98%); ^{1}H NMR (CDCl$_3$, 300 MHz) δ (ppm): 7.28–7.32 (dd, 1H), 7.13–7.16 (m, 2H), 7.05–7.09 (t, 1H), 6.86–6.92 (d, 1H), 2.40 (s, 3H); ^{13}C{^{1}H}(CDCl$_3$, 500 MHz) δ (ppm): 15.6, 109.8, 125.6, 129.7, 137.4.

2-Bromo-5-methylthiophene. Thiophene (200 mmol) and 200 mL of THF were cooled to −78 °C followed by dropwise addition of *n*-BuLi (200 mmol, 125 mL). MeI (240 mmol, 34.05 g) was added dropwise and stirred overnight. The crude material was flashed through an alumina plug with hexanes to yield 9.76 g of 2-methylthiophene (51%). The product (183.1 mmol, 17.98 g) was dissolved in 200 mL of DMF with NBS (183.1 mmol, 32.58 g) and stirred for 24 h. The crude product was distilled to yield 31 g of 2-bromo-5-methylthiophene (97%). Isopropylmagnesium chloride (175 mmol, 87.93 mL) was added dropwise to 2-bromothiophene (175 mmol, 28.53 g) in 100 mL of THF at 0 °C and stirred for 2 h. This solution was added dropwise to 2-bromo-5-methylthiophene (175 mmol, 30.98 g) and 3 mol % Ni(dppp)Cl$_2$ (5.25 mmol) in 140 mL of THF at 0 °C and stirred for 48 h. The reaction was quenched with

dx.doi.org/10.1021/jo402259z | J. Org. Chem. 2014, 79, 1836–1841

dilute HCl, and the solvent was removed. The crude mixture was dissolved in hexane, washed with water (3×) and brine (3×), and dried over $MgSO_4$. Distillation yielded 6.4 g (80% conversion) of coupled product along with 2,2′-dimethyl-2,2′-bithiophene, bithiophene, and starting material. ($A_f P_f$) = (6.40 g, 80%); ^{1}H NMR ($CDCl_3$, 300 MHz) δ (ppm): 7.06−7.10 (dd, 1H), 6.88−6.91 (t, 1H), 6.74−6.78 (dd, 1H), 2.51 (s, 3H). $^{13}C\{^1H\}$ ($CDCl_3$, 500 MHz) δ (ppm): 15.9, 109.1, 126.1, 130.1, 141.7.

Computational Methods. Modeling the intramolecular OA of a zerovalent nickel with haloarene substrates was done with density functional theory (DFT) using the B3LYP functional,[22] which yields accurate molecular geometries for transition-metal complexes.[23] All geometry optimizations and frequency computations used the 6-31G* basis set for H, C, O, P, and S[24,25] and the LANL2DZ basis set and effective core potential (ECP) for halogens and nickel.[26] Final energetics were computed with the B3LYP-D3 functional, which appends the Grimme dispersion correction[27] to B3LYP, along with a TZ2P basis set[28] contracted as (5*s*2*p*/3*s*2*p*) for H, (10*s*6*p*2*d*/5*s*3*p*2*d*) for C and O, and (14*s*10*p*2*d*/7*s*5*p*2*d*) for P and S, as well as the LANL2TZ(f) basis set and ECP for nickel and the LANL08d basis set and ECP for halogens.[29] This scheme is denoted as B3LYP-D3/TZ2P-LANL2TZ(f)-LANL08d. Electronic energies were corrected for zero-point vibrations. All computations employed a radial, angular (75, 302) grid with the QChem 4.0 package.[30] To validate our method, rigorous coupled-cluster computations were done for the complexation of Ni(dhpe) + ethene (Table S7). CCSD/TZ2P-LANL2TZ(f) gives a binding energy of 45.6 kcal mol^{-1}, similar to the 43.4 kcal mol^{-1} found by B3LYP-D3/TZ2P-LANL2TZ(f). Transition state theory (TST) was used to determine theoretical KIEs for nickel insertion.[12] Theoretical KIEs were benchmarked against experimental KIEs for the Diels−Alder reaction of *s-trans*-isoprene and maleic anhydride.[31]

■ ASSOCIATED CONTENT

Supporting Information

KIE determination, ^{13}C NMR spectra, benchmark of theoretical KIE calculations, benchmark of DFT energetics, total electronic energies, and optimized Cartesian coordinates of all stationary points. This material is available free of charge via the Internet at http://pubs.acs.org.

■ AUTHOR INFORMATION

Corresponding Authors

*E-mail: wdallen@uga.edu (W.D.A.).
*E-mail: jlocklin@uga.edu (J.L).

Author Contributions

‖These authors contributed equally.

Notes

The authors declare no competing financial interest.

■ ACKNOWLEDGMENTS

This work was supported by the National Science Foundation (CHE 1058631 and DMR 0953112).

■ REFERENCES

(1) (a) Tamao, K.; Sumitani, K.; Kumada, M. *J. Am. Chem. Soc.* **1972**, *94*, 4374. (b) Jana, R.; Pathak, T. P.; Sigman, M. S. *Chem. Rev.* **2011**, *111*, 1417. (c) Corriu, R. J. P.; Masse, J. P. *J. Chem. Soc., Chem. Commun.* **1972**, 144. (d) Yamamoto, T.; Wakabayashi, S.; Osakada, K. *J. Organomet. Chem.* **1992**, *428*, 223.

(2) (a) Churchill, D. G.; Janak, K. E.; Wittenberg, J. S.; Parkin, G. *J. Am. Chem. Soc.* **2003**, *125*, 1403. (b) Jones, W. D. *Acc. Chem. Res.* **2002**, *36*, 140. (c) Gómez-Gallego, M.; Sierra, M. A. *Chem. Rev.* **2011**, *111*, 4857.

(3) (a) Yoshikai, N.; Matsuda, H.; Nakamura, E. *J. Am. Chem. Soc.* **2008**, *130*, 15258. (b) Li, Z.; Jiang, Y.-Y.; Fu, Y. *Chem.—Eur. J.* **2012**, *18*, 4345. (c) Gøgsig, T. M.; Kleimark, J.; Nilsson Lill, S. O.; Korsager, S.; Lindhardt, A. T.; Norrby, P.-O.; Skrydstrup, T. *J. Am. Chem. Soc.* **2011**, *134*, 443. (d) McMullin, C. L.; Jover, J.; Harvey, J. N.; Fey, N. *Dalton Trans.* **2010**, *39*, 10833.

(4) Massera, C.; Frenking, G. *Organometallics* **2003**, *22*, 2758.

(5) Zenkina, O. V.; Karton, A.; Freeman, D.; Shimon, L. J. W.; Martin, J. M. L.; van der Boom, M. E. *Inorg. Chem.* **2008**, *47*, 5114.

(6) Bryan, Z. J.; McNeil, A. J. *Chem. Sci.* **2013**, *4*, 1620.

(7) (a) Sheina, E. E.; Liu, J.; Iovu, M. C.; Laird, D. W.; McCullough, R. D. *Macromolecules* **2004**, *37*, 3526. (b) Miyakoshi, R.; Yokoyama, A.; Yokozawa, T. *J. Am. Chem. Soc.* **2005**, *127*, 17542.

(8) Bridges, C. R.; McCormick, T. M.; Gibson, G. L.; Hollinger, J.; Seferos, D. S. *J. Am. Chem. Soc.* **2013**, *135*, 13212.

(9) Bryan, Z. J.; McNeil, A. J. *Macromolecules* **2013**, *46*, 8395.

(10) (a) Zenkina, O. V.; Karton, A.; Freeman, D.; Shimon, L. J. W.; Martin, J. M. L.; van der Boom, M. E. *Inorg. Chem.* **2008**, *47*, 5114. (b) Lanni, E. L.; Locke, J. R.; Gleave, C. M.; McNeil, A. J. *Macromolecules* **2011**, *44*, 5136.

(11) Vo, L. K.; Singleton, D. A. *Org. Lett.* **2004**, *6*, 2469.

(12) Smith, I. W. M. *Kinetics and dynamics of elementary gas reactions*; Butterworth & Co. Publishers Ltd.: Wobrun, MA, 1980.

(13) Singleton, D. A.; Thomas, A. A. *J. Am. Chem. Soc.* **1995**, *117*, 9357.

(14) Marshall, N.; Sontag, S. K.; Locklin, J. *Macromolecules* **2010**, *43*, 2137.

(15) Helm, L.; Merbach, A. E. *Chem. Rev.* **2005**, *105*, 1923.

(16) Seeman, J. I. *Chem. Rev.* **1983**, *83*, 83.

(17) Kozuch, S.; Shaik, S. *Acc. Chem. Res.* **2010**, *44*, 101.

(18) (a) Vechorkin, O.; Proust, V.; Hu, X. *J. Am. Chem. Soc.* **2009**, *131*, 9756. (b) Beryozkina, T.; Senkovskyy, V.; Kaul, E.; Kiriy, A. *Macromolecules* **2008**, *41*, 7817.

(19) (a) Tkachov, R.; Senkovskyy, V.; Komber, H.; Kiriy, A. *Macromolecules* **2011**, *44*, 2006. (b) Doubina, N.; Paniagua, S. A.; Soldatova, A. V.; Jen, A. K. Y.; Marder, S. R.; Luscombe, C. K. *Macromolecules* **2011**, *44*, 512.

(20) (a) Shi, L.; Chu, Y.; Knochel, P.; Mayr, H. *Org. Lett.* **2009**, *11*, 3502. (b) Shi, L.; Chu, Y.; Knochel, P.; Mayr, H. *J. Org. Chem.* **2009**, *74*, 2760. (c) Shi, L.; Chu, Y.; Knochel, P.; Mayr, H. *Org. Lett.* **2012**, *14*, 2602.

(21) (a) Alger, T. D.; Solum, M.; Grant, D. M.; Silcox, G. D.; Pugmire, R. J. *Anal. Chem.* **1981**, *53*, 2299. (b) Luukko, P.; Alvila, L.; Holopainen, T.; Rainio, J.; Pakkanen, T. T. *J. Appl. Polym. Sci.* **1998**, *69*, 1805.

(22) (a) Lee, C.; Yang, W.; Parr, R. G. *Phys. Rev. B* **1988**, *37*, 785. (b) Becke, A. D. *J. Chem. Phys.* **1993**, *98*, 5648.

(23) (a) Niu, S.; Hall, M. B. *Chem. Rev.* **2000**, *100*, 353. (b) Xu, Z.-F.; Xie, Y.; Feng, W.-L.; Schaefer, H. F. *J. Phys. Chem. A* **2003**, *107*, 2716.

(24) Dill, J. D.; Pople, J. A. *J. Chem. Phys.* **1975**, *62*, 2921.

(25) Francl, M. M.; Pietro, W. J.; Hehre, W. J.; Binkley, J. S.; Gordon, M. S.; DeFrees, D. J.; Pople, J. A. *J. Chem. Phys.* **1982**, *77*, 3654.

(26) Hay, P. J.; Wadt, W. R. *J. Chem. Phys.* **1985**, *82*, 299.

(27) Grimme, S.; Antony, J.; Ehrlich, S.; Krieg, H. *J. Chem. Phys.* **2010**, *132*, 154104.

(28) Gonzales, J. M.; Cox, R. S.; Brown, S. T.; Allen, W. D.; Schaefer, H. F. *J. Phys. Chem. A* **2001**, *105*, 11327.

(29) Roy, L. E.; Hay, P. J.; Martin, R. L. *J. Chem. Theory Comput.* **2008**, *4*, 1029.

(30) Shao, Y.; Fusti-Molnar, L.; Jung, Y.; Kussmann, J.; Ochsenfeld, C.; Brown, S. T.; Gilbert, A. T. B.; Slipchenko, L. V.; Levchenko, S. V.; O'Neill, D. P.; Distasio, R. A., Jr.; Lochan, R. C.; Wang, T.; Beran, G. J. O.; Besley, N. A.; Herbert, J. M.; Yeh Lin, C.; Van Voorhis, T.; Hung Chien, S.; Sodt, A.; Steele, R. P.; Rassolov, V. A.; Maslen, P. E.; Korambath, P. P.; Adamson, R. D.; Austin, B.; Baker, J.; Byrd, E. F. C.; Dachsel, H.; Doerksen, R. J.; Dreuw, A.; Dunietz, B. D.; Dutoi, A. D.; Furlani, T. R.; Gwaltney, S. R.; Heyden, A.; Hirata, S.; Hsu, C.-P.; Kedziora, G.; Khalliulin, R. Z.; Klunzinger, P.; Lee, A. M.; Lee, M. S.; Liang, W.; Lotan, I.; Nair, N.; Peters, B.; Proynov, E. I.; Pieniazek, P. A.; Min Rhee, Y.; Ritchie, J.; Rosta, E.; David Sherrill, C.; Simmonett, A. C.; Subotnik, J. E.; Lee Woodcock, H., III; Zhang, W.; Bell, A. T.; Chakraborty, A. K.; Chipman, D. M.; Keil, F. J.; Warshel, A.; Hehre,

W. J.; Schaefer, H. F., III; Kong, J.; Krylov, A. I.; Gill, P. M. W.; Head-Gordon, M. *Phys. Chem. Chem. Phys.* **2006**, *8*, 3172.
(31) Beno, B. R.; Houk, K. N.; Singleton, D. A. *J. Am. Chem. Soc.* **1996**, *118*, 9984.